

Supporting Information

Activatable Photothermal Agents With Target-initiated Large Spectral Separation for Highly Effective Reduction of Side Effects

Jie Sun,^{‡a} Ning Cheng,^{‡a} Kai Yin,^{‡b} Rongchen Wang,^a Tianli Zhu,^a Jinzhu Gao,^a
Xuemei Dong,^a Chengjun Dong,^a Xianfeng Gu,^{*b} Chunchang Zhao^{*a}

^a Key Laboratory for Advanced Materials and Feringa Nobel Prize Scientist Joint Research Center, Institute of Fine Chemicals, School of Chemistry and Molecular Engineering, Frontiers Science Center for Materiobiology and Dynamic Chemistry, East China University of Science and Technology, Shanghai 200237, China

^b Department of Medicinal Chemistry, School of Pharmacy, Fudan University, Shanghai 201203, China

[‡] These authors contributed equally.

* Corresponding authors: Prof. C. Zhao, E-mail: zhaocchang@ecust.edu.cn; Prof. X. Gu, E-mail: xfgu@fudan.edu.cn

condition, followed by dropwise addition of p-methylphenylcyclochloride (19.06 g, 0.1 mol) in THF (50 mL). After stirring in ice bath for 2h, the reaction mixture was extracted with CH₂Cl₂, washed with aqueous NaOH (1 M) and water. Then, the organic phase was dried with anhydrous Na₂SO₄, evaporated and concentrated to obtain colorless oily liquid compound 1. ¹H NMR (400 MHz, CDCl₃, δ): 7.77 (d, 2 H), 7.34 (d, 2H), 4.14 (t, 2 H), 3.67 (t, 2 H), 3.60-3.58 (m, 6H), 3.51 (d, 2 H), 3.36 (s, 3 H), 2.36 (s, 3 H).

Synthesis of compound 2: Compounds 1 (10 g, 0.0314 mol), p-hydroxy benzaldehyde (4.23 g, 0.0314 mol) and K₂CO₃ (4.33 g, 0.0314 mol) were both dissolved in DMF (25 mL), and the solution was heated under reflux for 6 h. After evaporating the solvent, the residue was dissolved in CH₂Cl₂, washed with brine, dried over anhydrous Na₂SO₄, and filtered. The crude mixture was purified by column chromatography on silica gel (PE/EA, 20: 1, v/v) to afford compound 2 as a colorless liquid. ¹H NMR (400 MHz, CDCl₃, δ): 9.90 (s, 1 H), 7.85 (d, 2 H), 7.04 (d, 2 H), 4.24 (t, 2 H), 3.91 (t, 2 H), 3.75 (t, 2 H), 3.70 (t, 2 H), 3.66 (t, 2 H), 3.56 (t, 2 H), 3.39 (s, 3 H).

Synthesis of compound 3: Compound 2 (5 g, 0.0186 mol) in ethanol (25 mL) was treated with NaOH (18 mL, 0.05 M) under an ice-cooling condition, followed with 4-N, N-dimethylacetophenone (3.34 g, 0.0205 mol) added into the solution. The mixture was stirred for 6 h at room temperature. Then, the mixture was extracted by CH₂Cl₂, dried with anhydrous Na₂SO₄. The organic solvent was removed and the crude product was purified by silica gel column chromatography, in which a yellow solid product compound 3 was obtained. ¹H NMR (400 MHz, CDCl₃, δ): 8.02 (d, 2 H), 7.73 (d, 1 H), 7.57 (d, 2 H), 7.45 (d, 1 H), 6.93 (d, 2 H), 6.72 (d, 2 H), 4.17 (t, 2 H), 3.87 (t, 2 H), 3.74 (t, 2 H), 3.69 (t, 2 H), 3.65 (d, 2 H), 3.55 (t, 2 H), 3.38 (s, 3 H), 3.08 (s, 6 H).

Synthesis of compound 4: Compound 3 (3 g, 7.26 mmol) in ethanol (25 mL) was treated with 20% KOH (2.5 mL) aqueous solution and nitromethane (5.7 mL, 0.1089 mol). The reaction mixture was refluxed for 5 h. The organic solvent was removed and the crude product was purified by silica gel flash chromatography to provide compound

4. ¹H NMR (400 MHz, CDCl₃, δ): 7.85 (d, 2H), 7.19 (d, 2H), 6.89 (d, 2H), 6.72 (d, 2H), 4.83 (m, 1H), 4.65 (m, 1H), 4.18 (m, 1H), 4.12 (t, 2H), 3.85 (t, 2H), 3.75 (t, 2H), 3.70 (d, 2H), 3.67 (d, 2H), 3.58 (s, 2H), 3.40 (s, 3H), 3.34 (s, 2H), 3.09 (s, 6H).

Synthesis of compound aza-BODIPY-1: Compound 4 (1 g, 2.1 mmol) and ammonium acetate (2.42 g, 31.5 mmol) were dissolved in butyl alcohol (10 mL), and the reaction mixture was refluxed for 4 h. After evaporating the solvent, the residue was washed with cooled methanol, which obtained a green product that was used in the next reaction directly. The green product was dissolved in dry dichloromethane (20 mL), added diisopropylethylamine (1.734 mL, 15 mmol) and boron trifluoride etherate (2.64 mL, 21 mmol) successively. After being stirred overnight at room temperature, the mixture was extracted with CH₂Cl₂. The organic layer was separated and dried over anhydrous Na₂SO₄. The organic solvent was removed and the crude product was purified by silica gel column chromatography (DCM/MeOH, 50:1, v/v), which has a red metallic power (aza-BODIPY-1) afforded. ¹H NMR (400 MHz, DMSO-*d*₆, δ): 8.22 (m, 8H), 7.55 (s, 2H), 7.16 (d, 4H), 6.91 (d, 4H), 4.26 (t, 4H), 3.85 (t, 4H), 3.65 (t, 4H), 3.61 (t, 4H), 3.57 (t, 4H), 3.46 (t, 4H), 3.39 (s, 6H), 3.14 (s, 12H). ¹³C NMR (400 MHz, DMSO-*d*₆, δ): 159.25, 154.67, 151.66, 143.75, 139.19, 131.48, 130.14, 125.05, 117.84, 117.05, 114.63, 111.77, 71.23, 70.65, 68.95, 68.90, 67.24, 58.00. HRMS (ESI, m/z) calculated for C₅₀H₆₀BF₂N₅O₈ [M + Na]⁺: 930.440, found: 930.4395.

Synthesis of compound aza-BOD-B1 and aza-BOD-B2: Compound 5 (200 mg, 0.178 mmol) and 4-bromomethylphenylboronic acid pinacol ester (53 mg, 0.178 mmol) were dissolved in dry acetonitrile (20 mL). The reaction mixture was refluxed for 24 h. After the evaporated solvent, the crude product was purified by column chromatography (H₂O/MeOH, 3:7, v/v), which aza-BOD-B1 and aza-BOD-B2 were obtained respectively. aza-BOD-B1: ¹H NMR (400 MHz, DMSO-*d*₆, δ): 8.41 (d, 2H), 8.26 (d, 2H), 8.18 (d, 2H), 8.08 (d, 2H), 8.00 (d, 2H), 7.98 (s, 1H), 7.74 (d, 2H), 7.29 (s, 1H), 7.17 (d, 2H), 7.11 (t, 4H), 6.91 (d, 2H), 5.09 (s, 2H), 4.21 (d, 4H), 3.80 (t, 4H), 3.64 (t, 4H), 3.61 (t, 4H), 3.56 (t, 4H), 3.54 (t, 4H), 3.44 (t, 6H), 3.24 (s, 6H), 3.20 (s, 6H), 1.23 (s, 12H). ¹³C NMR (400 MHz, CDCl₃, δ): 134.86, 129.90, 114.60, 111.76, 70.86, 67.38,

69.62, 67.21, 59.01, 45.72, 31.92, 29.52, 29.11, 24.83, 22.70, 14.18. HRMS (ESI, m/z) calculated for $C_{63}H_{78}B_2F_2N_5O_{10}^+$ [M]⁺:1124.5891, found: 1124.5881. aza-BOD-B2: ¹H NMR (400 MHz, DMSO-*d*₆, δ): 8.29 (d, 2H), 8.21 (d, 6H), 8.09 (d, 4H), 7.72 (d, 4H), 7.68 (s, 2H), 7.23 (d, 4H), 7.09 (d, 4H), 5.11 (s, 4H), 4.26 (t, 4H), 3.81 (t, 4H), 3.65 (t, 4H), 3.62 (t,4H), 3.56 (t, 4H), 3.53 (t, 4H), 3.44 (s, 6H), 3.23 (s, 12H). ¹³C NMR (600 MHz, DMSO-*d*₆, δ): 162.37, 161.13, 160.79, 159.18, 154.38, 148.45, 146.62, 145.76, 144.89, 139.72, 134.82, 134.70, 134.41, 132.03, 131.62, 131.33, 130.18, 130.05, 129.89, 128.25, 125.83, 123.00, 122.30, 115.66, 115.31, 115.20, 71.74, 70.44, 70.28, 70.08, 58.52, 46.63. HRMS (ESI, m/z) calculated for $C_{64}H_{76}B_3F_2N_5O_{12}^{2+}$ [M]²⁺:588.7863, found: 588.7879.

3 · Cells culture and imaging.

A549 cells and HEK-293T cells were cultured at 37 °C in a humidified atmosphere of 5% CO₂ incubator within Roswell Park Memorial Institute 1640 medium (RPMI-1640) and DMEM medium containing 10% fetal bovine serum (FBS) and 1% penicillin-streptomycin, respectively. All cells were seeded in a cell culture flask and allowed to adhere for 24 hours before the experiment. For examination of cell death induced by aza-BOD-B2 mediated PTT, four groups A549 cells were cultured and treated respectively: 1) cells were incubated with aza-BOD-B2 (20 μM) for 3 h; 2) cells were irradiated with NIR laser (808 nm, 1.2 W cm⁻²) for 10 mins; 3) cells were incubated with aza-BOD-B2 (20 μM) for 3 h and then exposed to NIR laser light (808 nm, 1.2 W cm⁻²) for 10 mins; 4) untreated cells; all the four group of cells were stained with Calcein-AM (2 μM) and PI (4.5 μM) for 15 min at 37 °C, and performed by confocal imaging. The excitation wavelengths for Calcein-AM and PI were 488 nm and 561 nm, respectively. And the emission was collected between 490-540 nm and 592-642 nm for Calcein-AM and PI, respectively.

4 · Photothermal cytotoxicity in vitro.

A549 cells or HEK-293T cells seeded into 96-well plates were incubated with aza-BOD-B2 in different concentrations (0, 5, 10, 20, and 30 μM) for 3 h. After washing with a fresh culture medium, A549 cells or HEK-293T were exposed to NIR laser light

(808 nm, 1.2 W cm⁻²) for 10 min. The relative cell viability under dark and light irradiation was then assessed by the CCK-8 (10 μL) solution was added to the hatch for 1 h at 37 °C. The absorption spectrum was measured at 450 nm by using a microplate reader. The absorption of cells treated with PBS (control group) was used as the reference value for calculating 100% cellular viability. VR can be calculated using Equation (1)

$$VR = \frac{A - A_{\text{blank}}}{A_0 - A_{\text{blank}}} \times 100\% \quad (1)$$

In the above equation, A as an experimental group, A₀ as a control group, A_{Blank} as a blank group, the cytotoxic effect was obtained.

5、 Animal model.

All animal experiments were carried out in compliance with the relevant laws and institutional guidelines for the Care and Use of Research Animals established by Fudan University which approved the experimental protocols and procedures. Subcutaneous injection of A549 cells (4.0 × 10⁶) suspended in 200 μL to the indicated location in male nude mice (4 - 5 weeks) was performed to establish the xenograft A549 tumor-bearing mouse model. The mice with tumor size at about 40 - 50 mm³ were used subsequently for PTT experiments.

6、 In vivo PTT.

A549 tumor-bearing male nude mice were divided into five groups (5 mice per group): 1) untreated mice; 2) mice with aza-BOD-B2 (100 μL, 1.2 mg mL⁻¹) injection into tumors but no laser irradiation; 3) mice with laser irradiation but no aza-BOD-B2 administration; 4) mice with both aza-BOD-B2 injection into tumors and laser irradiation; 5) normal mice with both aza-BOD-B2 injection and laser irradiation. For PTT, the tumor sites were irradiated with an 808 nm laser (1.2 W cm⁻²). IR images of mice were monitored by a thermal imaging camera as irradiation proceeded. After PTT treatment, the tumor size and body weight were monitored for 15 days. The mice were euthanized after 15 d and tumor samples were collected. The width and length of the tumors were measured with Vernier calipers. Tumor volume was estimated using the

following formula: tumor volume = $\pi/6 \times (\text{length} \times \text{width})^{3/2}$.

7、HE Analysis.

Paraffin-embedded sections were deparaffinized and hydrated. Hematoxylin solution was added to cover the slides; after staining for 3 min., the slides were washed with saline to remove excess hematoxylin staining solution. The slides were immersed in the differentiation solution for 3 s, and then washed in running water. The slides were exposed to the blue liquid for a total of 3 s. The slides were incubated with eosin for an additional 3 min. and then rinsed with saline. The nucleus was stained blue with hematoxylin, and the cytoplasm was stained red with eosin. The cells were observed using light microscopy.

8、Time-dependent absorption changes of aza-BOD-B2 in the presence of H₂O₂.

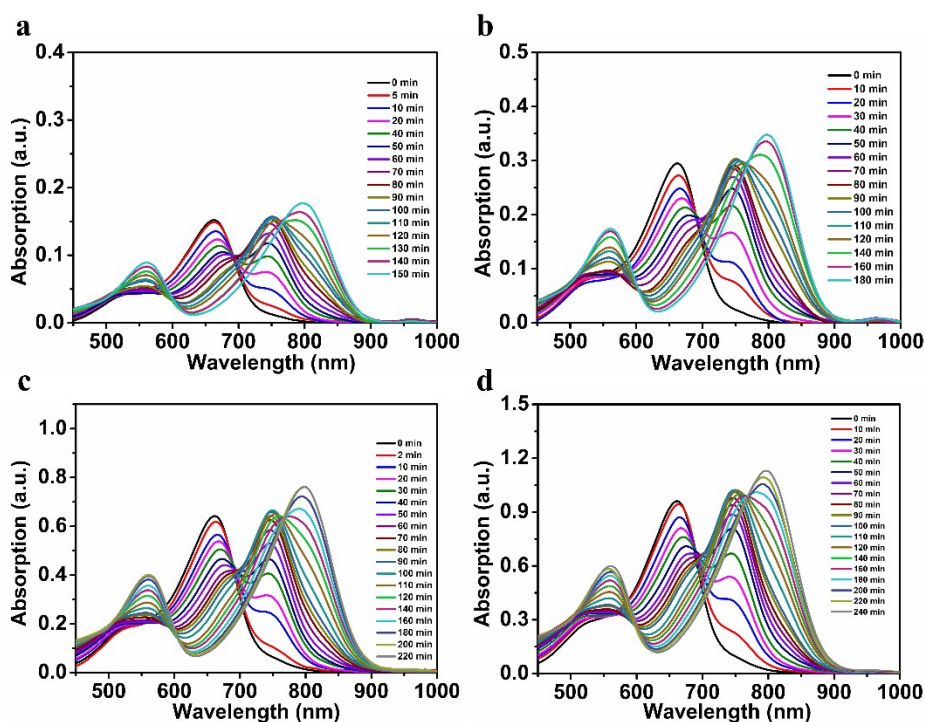


Figure S1. Time-dependent absorption changes of aza-BOD-B2 in the presence of 300 μM H₂O₂. (a) 5 μM , (b) 10 μM , (c) 20 μM , (d) 30 μM .

9、HMRS analysis.

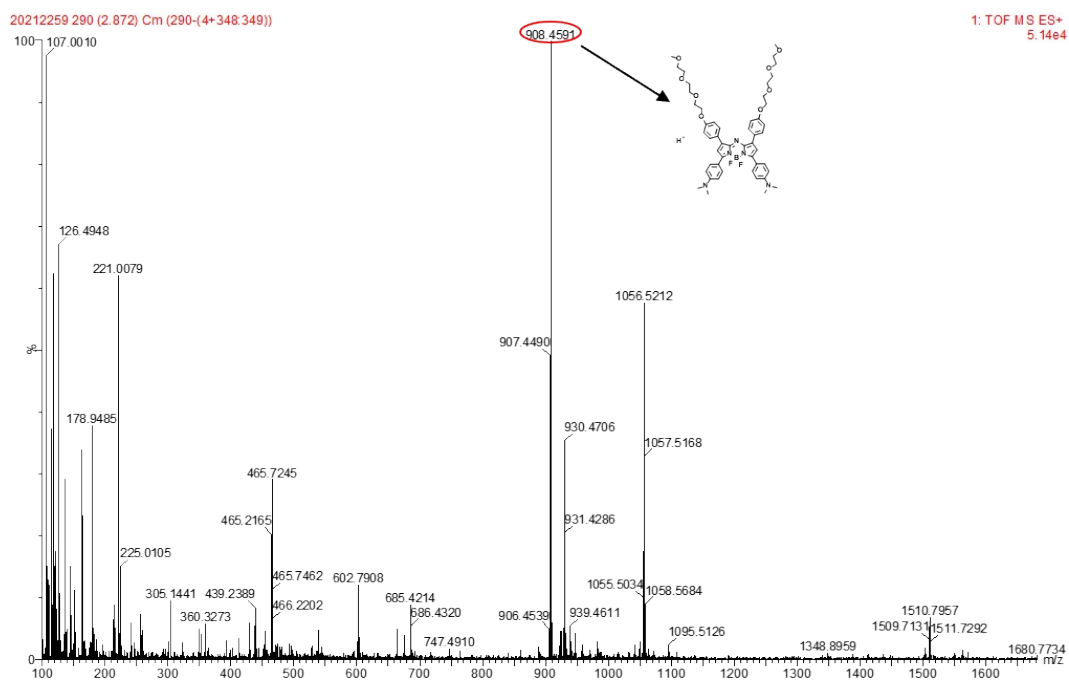


Figure S2. HRMS spectrum of the products from the reaction of aza-BOD-B2 with H_2O_2 .

10 · The pH and selectivity of aza-BOD-B1.

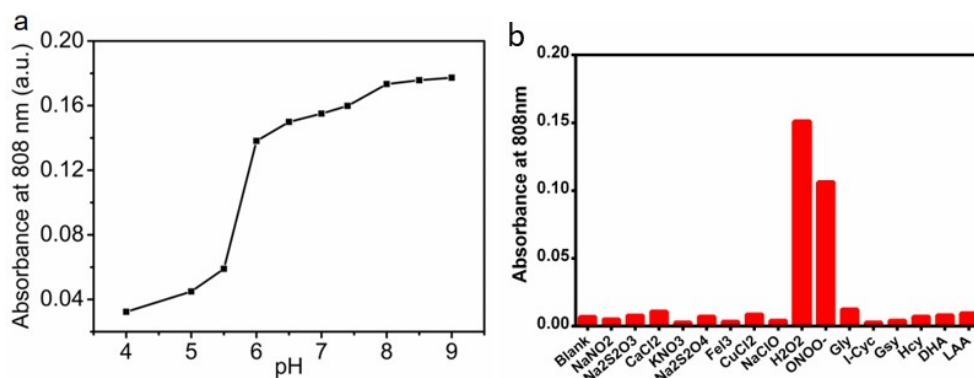


Figure S3. (a) The absorption intensity of aza-BOD-B2 ($5 \mu\text{M}$) reacts with H_2O_2 ($100 \mu\text{M}$) at 808 nm changes with pH (4 - 9). (b) Absorption intensity comparison of aza-BOD-B2 ($5 \mu\text{M}$) at $\lambda_{808 \text{ nm}}$ after adding 1 mM H_2O_2 or other active substances (NO_2^- , $\text{S}_2\text{O}_3^{2-}$, Ca^{2+} , NO_3^- , $\text{S}_2\text{O}_4^{2-}$, Fe^{3+} , Cu^{2+} , ClO^- , ONOO^- , Gly, L-cys, Gsy, Hcy, DHA, LAA).

11 · The pH and selectivity of aza-BOD-B2.

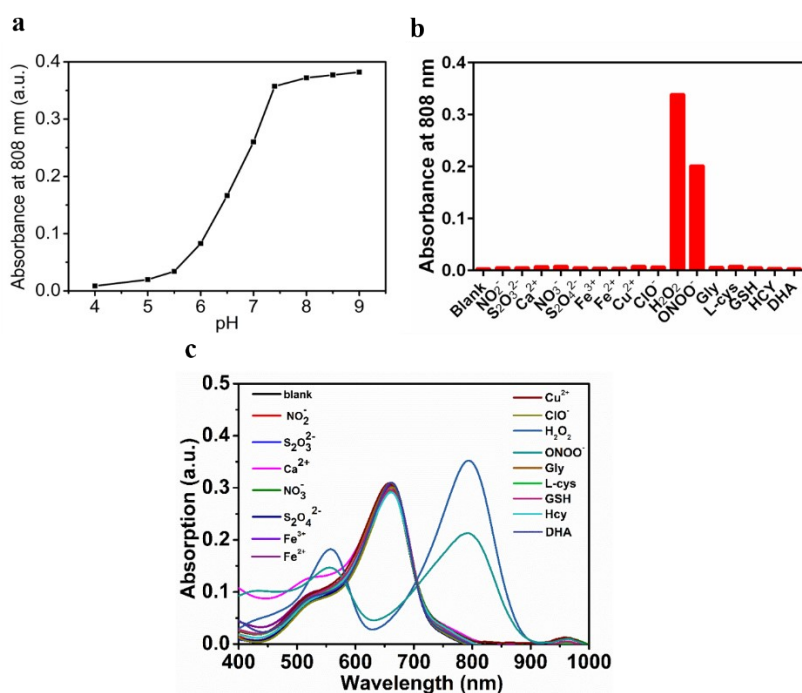


Figure S4. (a) The absorption intensity of aza-BOD-B2 (10 μM) reacts with H₂O₂ (200 μM) at 808 nm changes with pH (4 - 9); (b) The absorption intensity comparison of aza-BOD-B2 (10 μM) at $\lambda_{808 \text{ nm}}$ after adding 1 mM H₂O₂ or other active substances (NO₂⁻, S₂O₃²⁻, Ca²⁺, NO₃⁻, S₂O₄²⁻, Fe³⁺, Fe²⁺, Cu²⁺, ClO⁻, ONOO⁻, Gly, L-cys, GSH, Hcy, DHA). (c) The absorption spectrum of aza-BOD-B2 in the presence of different substances.

12 · The limit of detection (LOD) of aza-BOD-B1 and aza-BOD-B2.

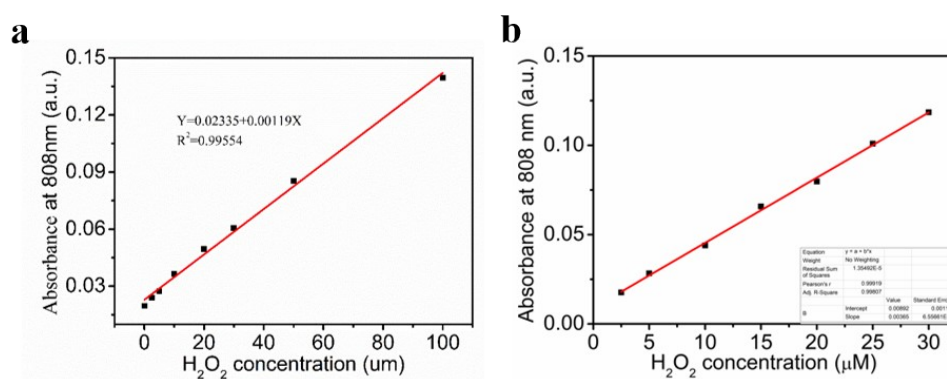


Figure S5. The absorbance at $\lambda_{808 \text{ nm}}$ changes of aza-BOD-B1 (5 μM) (a) and aza-BOD-B2 (10 μM) (b) as a function of H₂O₂ concentrations, which showed a good linear relationship as the concentration of H₂O₂ increased.

13 · Photothermal conversion efficiency.

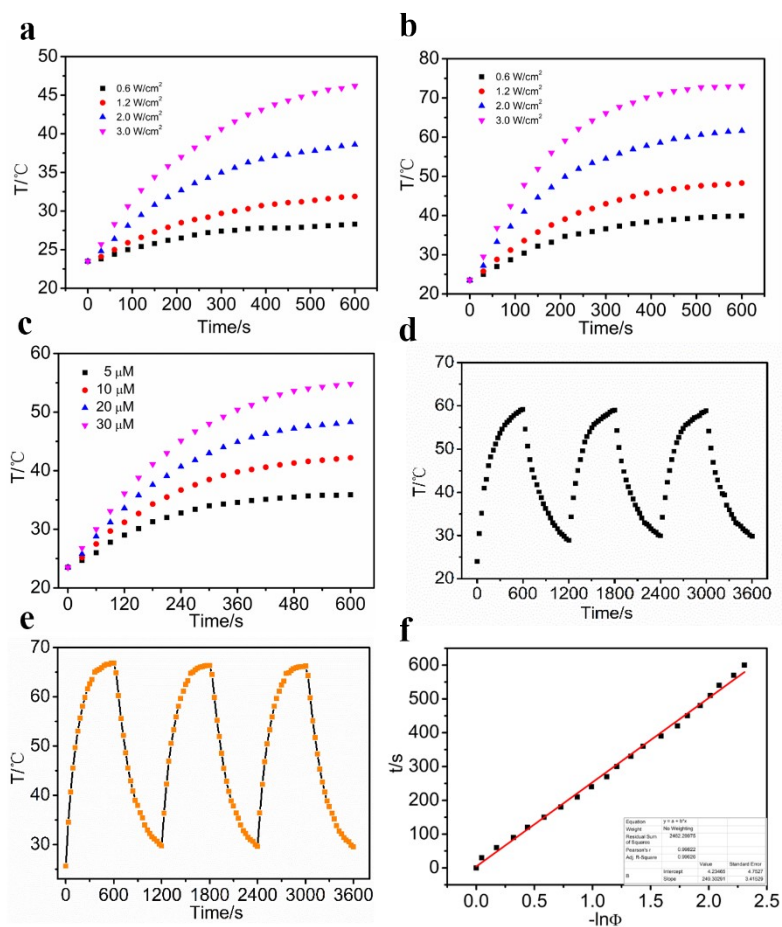


Figure S6. Laser-power-dependent temperature changes of aza-BOD-B1 (20 μM) in the absence of H_2O_2 (a) and in the presence of H_2O_2 (100 μM) (b); (c) Temperature elevation for aza-BOD-B1 at different concentrations in the presence of H_2O_2 (100 μM) under 808 nm laser irradiation (1.3 W cm^{-2}); The temperature changes of aza-BOD-B1 (20 μM) (d) and aza-BOD-B2 (20 μM) (e) in the presence of H_2O_2 (200 μM) upon cyclic photothermal heating and cooling processes; the cycle was performed by laser irradiation for 10 min, then naturally cooling to room temperature. (f) Relationship between t and $-\ln\theta$ of aza-BOD-B2.

The calculation method of light-to-heat conversion efficiency is as follows:

First, θ is the driving temperature calculated according to Equation (2)

$$\theta = \frac{T - T_{surr}}{T_{max} - T_{surr}} \quad (2)$$

T is the temperature corresponding to different irradiation time, T_{max} is the highest temperature of the solution after irradiation for 10 min, and T_{surr} is the initial temperature of the solution.

Next, τ_s (the associated time constant of the experimental system), can be calculated according to Equation (3):

$$t = -\tau_s \ln \theta \quad (3)$$

t is the time period corresponding to the cooling of the system after laser irradiation.

$$hS = \frac{mc}{\tau_s} \quad (4)$$

$$\eta = \frac{hS(T_{max} - T_{surr}) - Q_{dis}}{I(1 - 10^{-A_\lambda})} \quad (5)$$

Accordingly, the photothermal conversion efficiency (η) was determined according to a reported method.¹ Q_{dis} represents the heat dissipation of solvent which was measured by a power meter (VLP-2000). I is the laser power and A_λ is the absorbance at 808 nm. hS can be calculated according to Equation (4).

14、 Time-dependent temperature change curves of aza-BOD-B1 and aza-BOD-B2 after H₂O₂ activation.

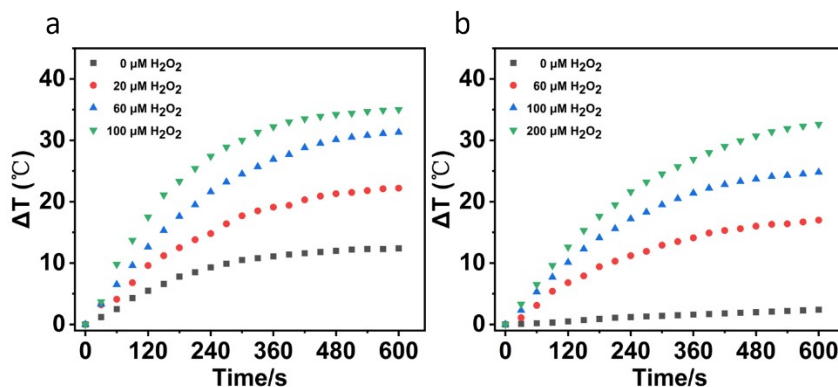


Figure S7. The temperature changes of aza-BOD-B1 (a) and aza-BOD-B1 (b) upon reacting with H₂O₂ at different concentrations under 808 nm laser irradiation (2 W cm⁻²).

15 · The photostability of aza-BOD-B1 and aza-BOD-B2.

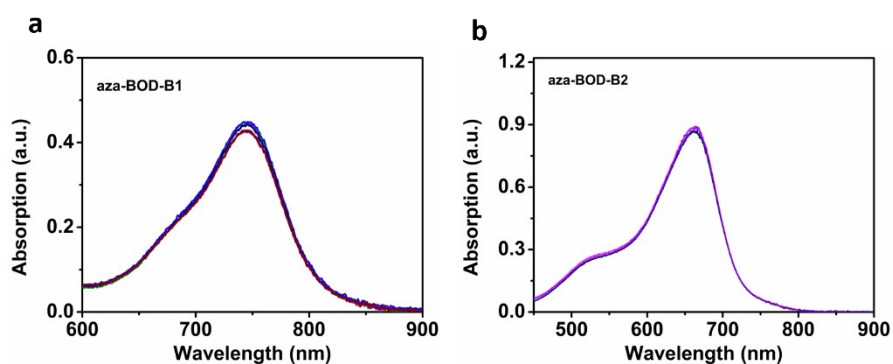


Figure S8. The absorption changes of aza-BOD-B1 (a) and aza-BOD-B2 (b) under continuous irradiation with an 808 nm laser (1.2 W cm^{-2}).

16 · Inhibitory assay by N-acetylcysteine (NAC) at the cellular level.

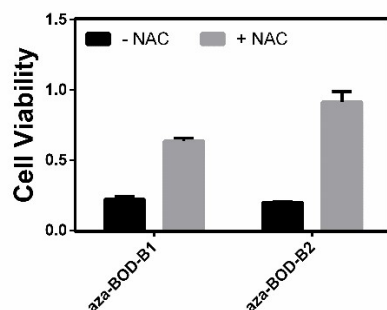


Figure S9. Viability of A549 cells incubated with aza-BOD-B1 ($30 \mu\text{M}$) and aza-BOD-B2 ($30 \mu\text{M}$) in the presence or absence of NAC (20 mM , 2 h) under irradiation with an 808 nm laser (1.2 W cm^{-2}), data are represented as mean \pm SD ($n = 3$).

17 · In vivo treatment outcome of the photothermal therapy with aza-BOD-

B2.

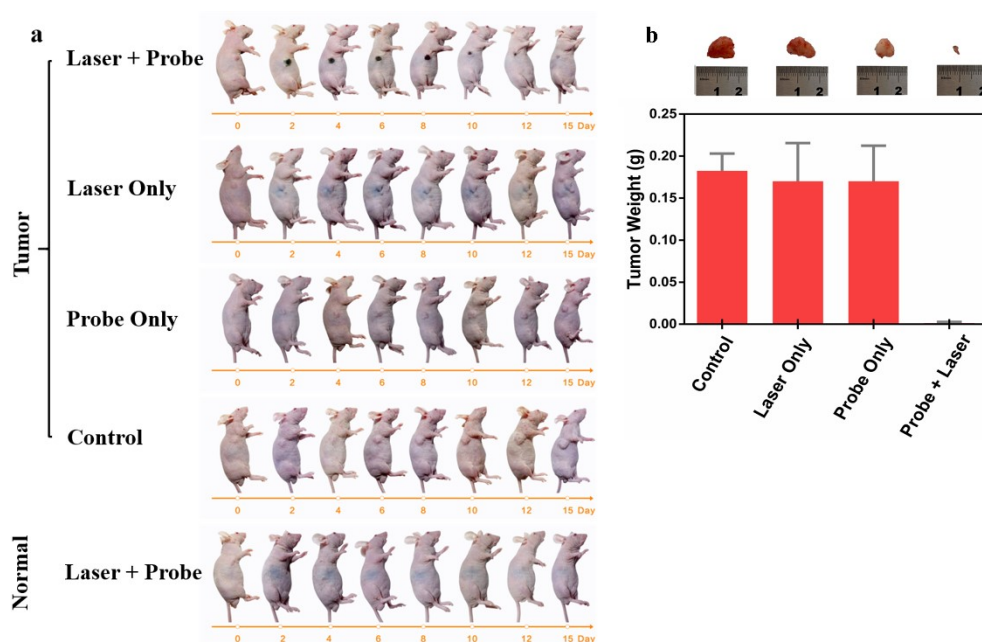


Figure S10. (a) Photos of untreated mice 808 nm laser irradiation with a power density of 1.2 W cm^{-2} was performed at 4 h post-administration of aza-BOD-B2 ($100 \mu\text{L}$, 1.2 mg mL^{-1}); (b) Tumor weight in different groups was obtained on day 15 and the representative photographs of tumor tissues on day 15. Data are represented as mean \pm SD ($n = 5$).

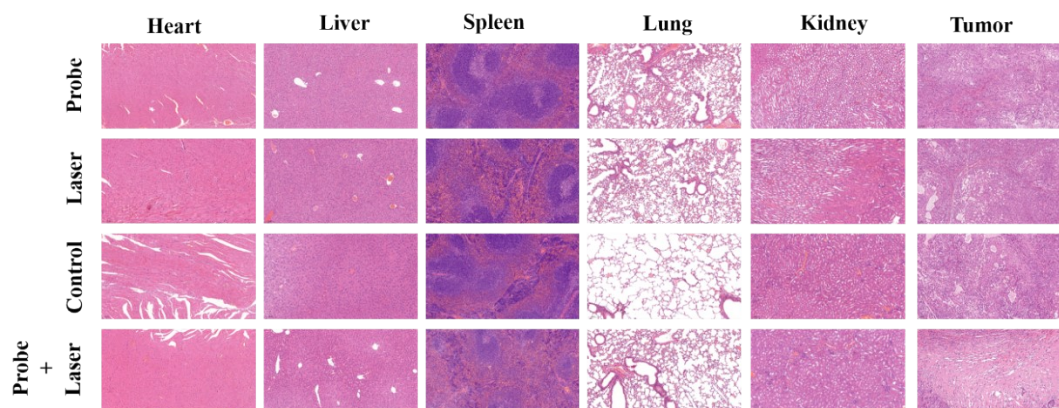


Figure S11. H&E staining for tumors of mice after various treatments and major organs of mice without treatment and treated with aza-BOD-B2 and 808 nm light irradiation. Scale bar = $100 \mu\text{m}$.

18 · NMR and HRMS characterization.

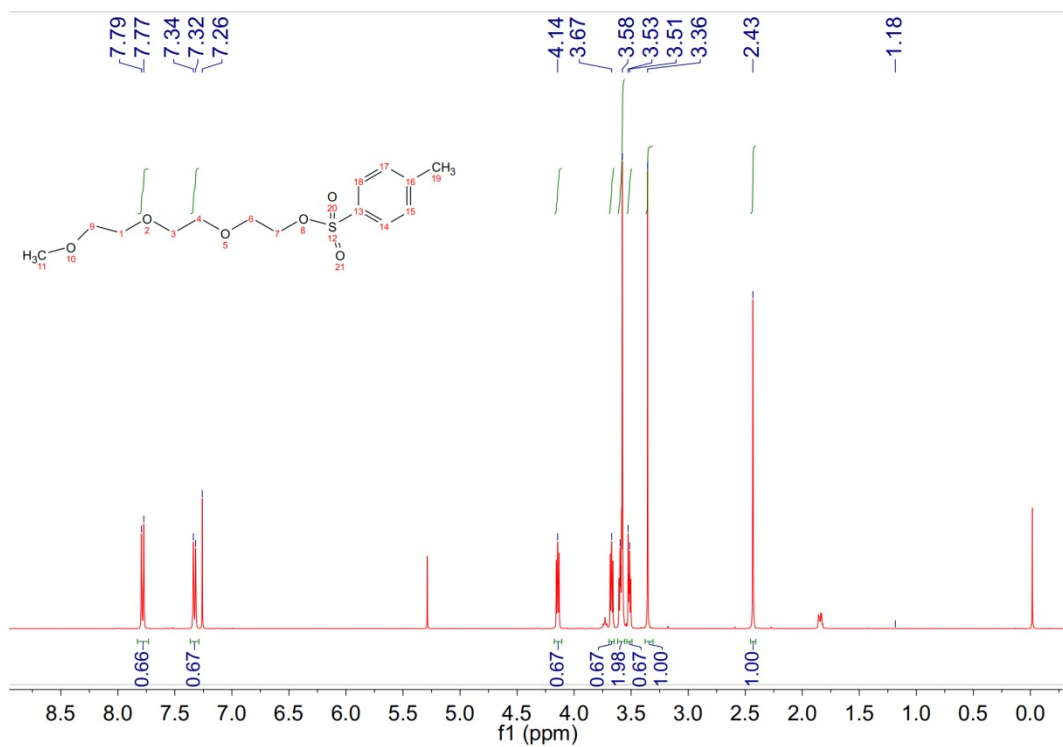


Figure S12. ^1H NMR (CDCl_3 , 400 MHz) spectrum of compound 1

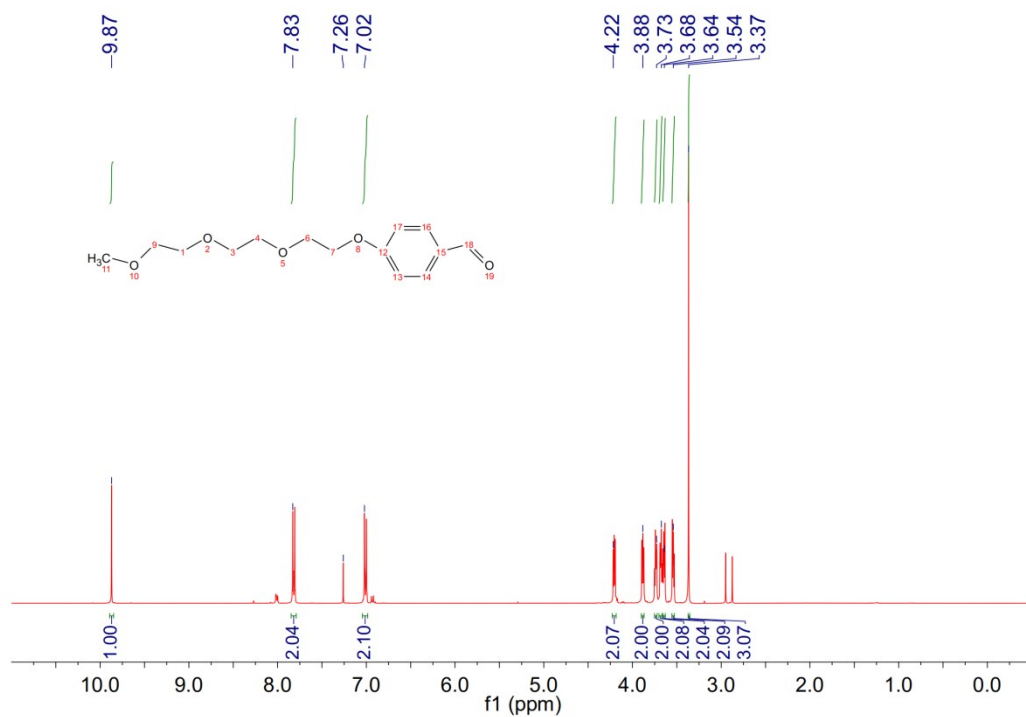


Figure S13. ^1H NMR (CDCl_3 , 400 MHz) spectrum of compound 2.

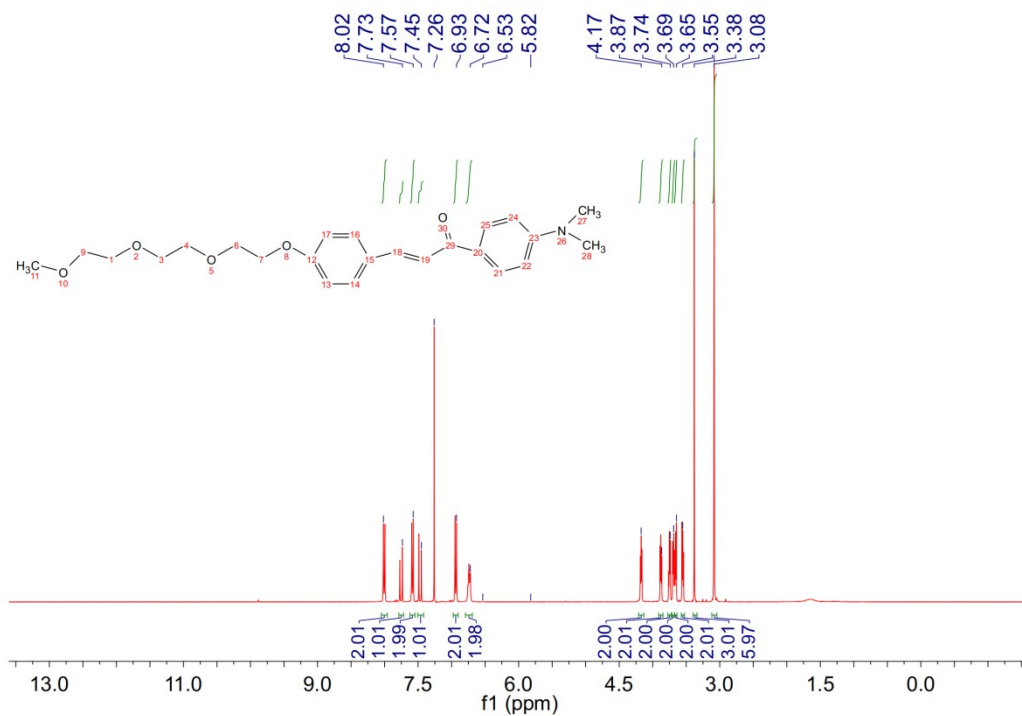


Figure S14. ¹H NMR (CDCl₃, 400 MHz) spectrum of compound 3

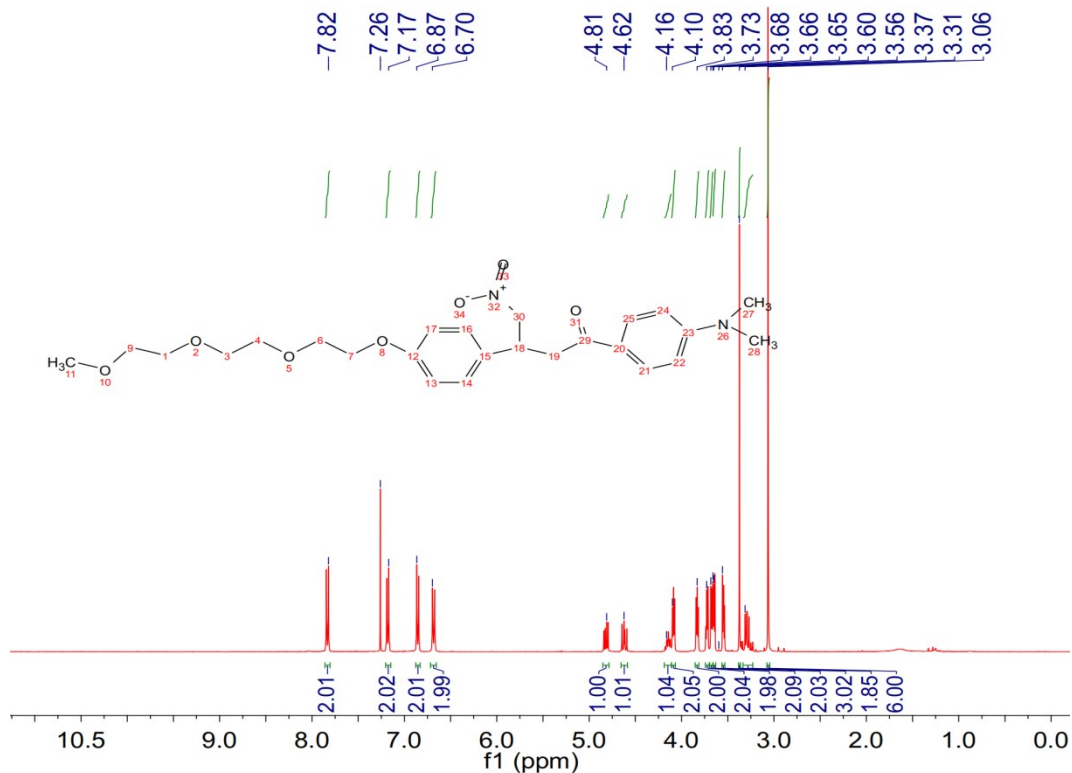


Figure S15. ¹H NMR (CDCl₃, 400 MHz) spectrum of compound 4

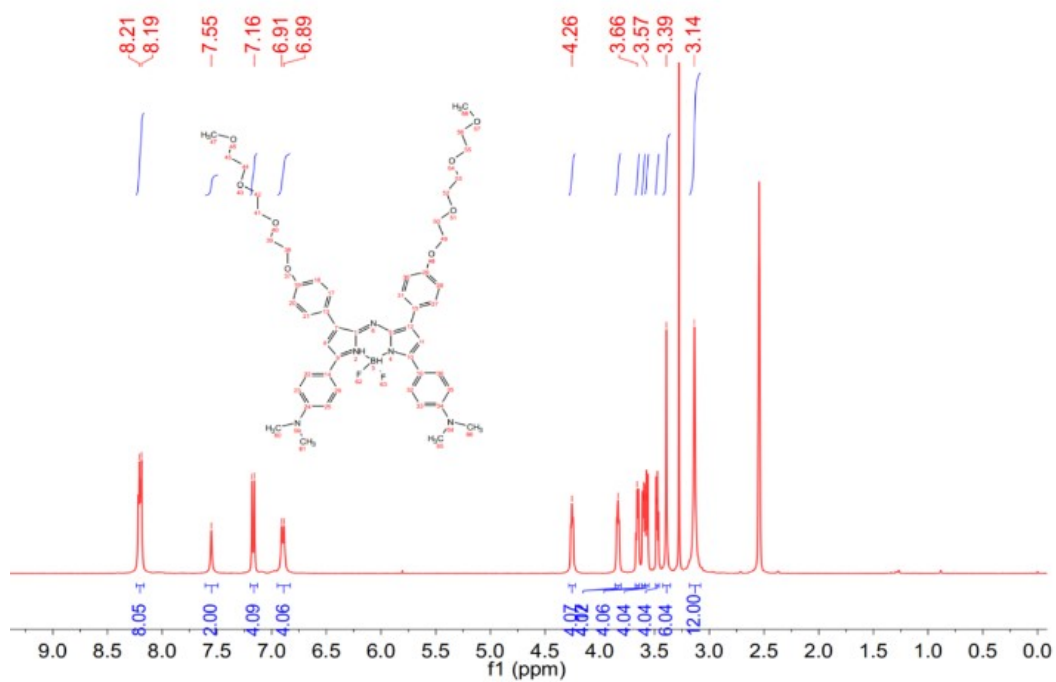


Figure S16. ^1H NMR ($\text{DMSO-}d_6$, 400 MHz) spectrum of compound aza-BODIPY-1

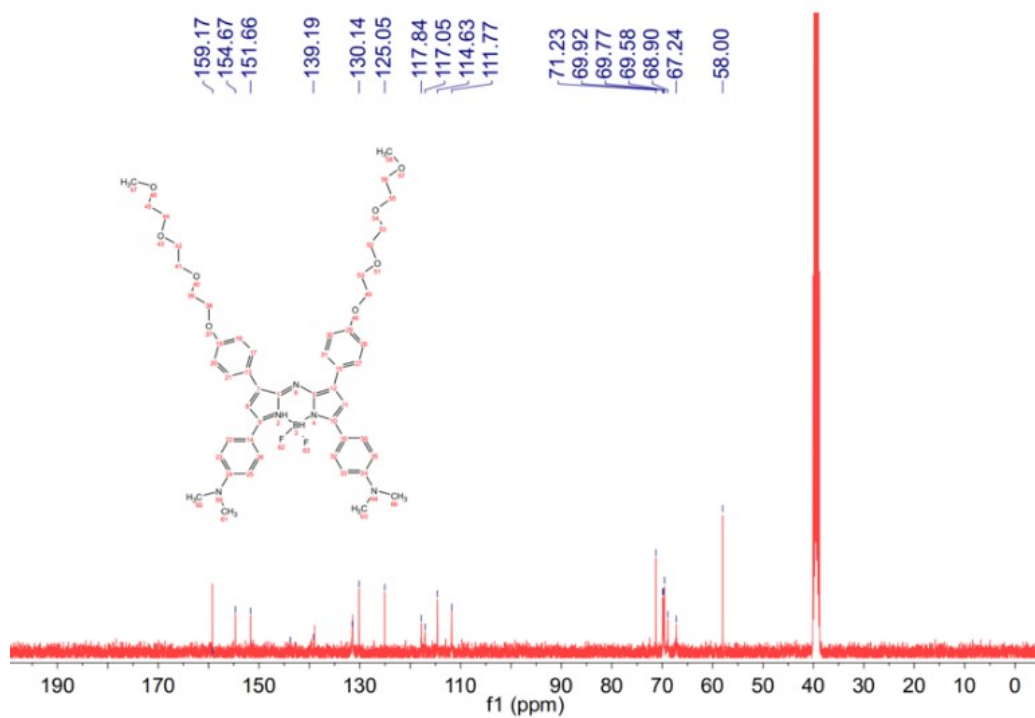


Figure S17. ^{13}C NMR ($\text{DMSO-}d_6$, 400 MHz) spectrum of compound aza-BODIPY-1

Single Mass Analysis

Tolerance = 5.0 PPM / DBE: min = -1.5, max = 50.0

Element prediction: Off

Number of isotope peaks used for i-FIT = 3

Monoisotopic Mass, Even Electron Ions

608 formula(e) evaluated with 1 results within limits (up to 50 best isotopic matches for each mass)

Elements Used:

C: 0-50 H: 0-70 N: 0-5 O: 0-8 Na: 0-1 F: 0-2 B: 0-1

CC-ZHAO

ZC-CN-13 47 (0.527) Cm (43:51)

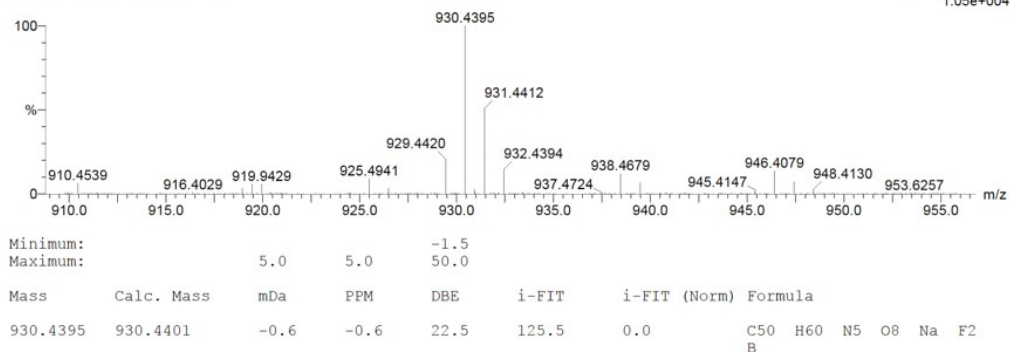
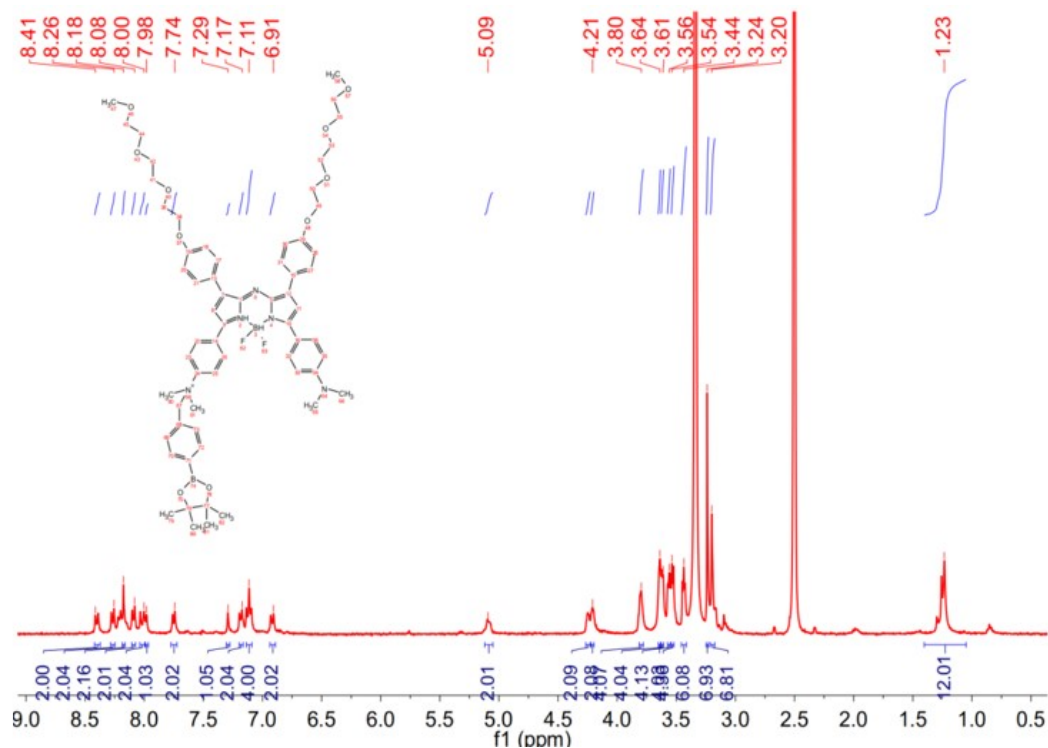
1: TOF MS ES+
1.05e+004

Figure S18. HRMS spectrum of compound aza-BODIPY-1

Figure S19. ¹H NMR (DMSO-*d*₆, 400 MHz) spectrum of compound aza-BOD-B1

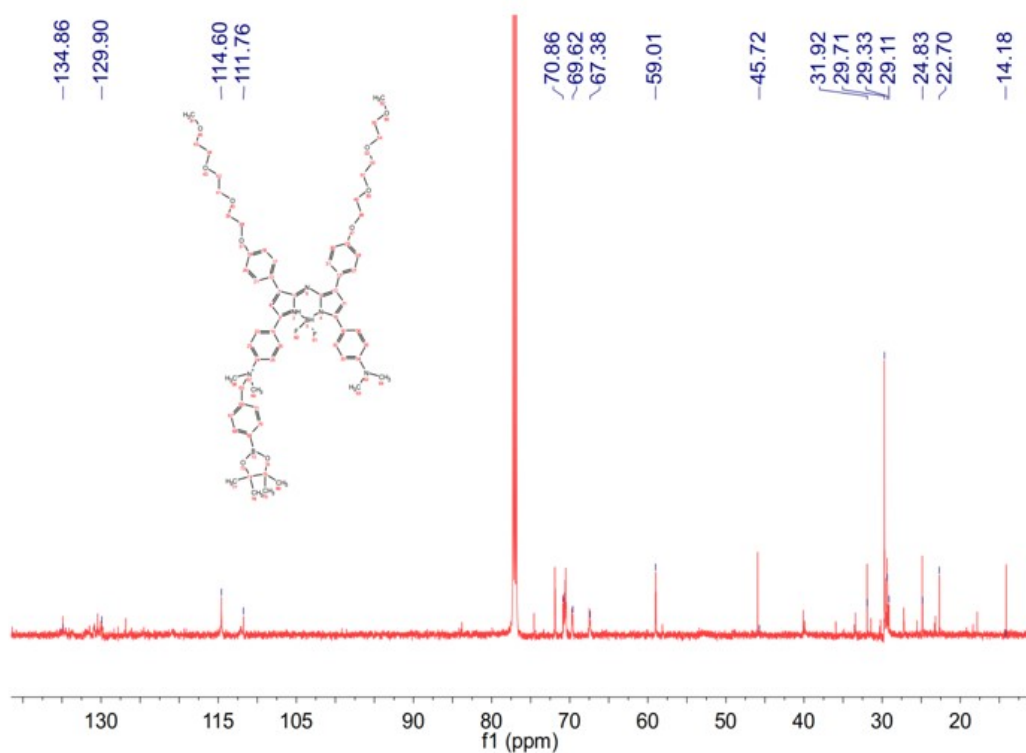


Figure S20. ^{13}C NMR (CDCl_3 , 400 MHz) spectrum of compound aza-BOD-B1

Elemental Composition Report

Page 1

Single Mass Analysis

Tolerance = 5.0 PPM / DBE: min = -1.5, max = 50.0

Element prediction: Off

Number of isotope peaks used for i-FIT = 3

Monoisotopic Mass, Even Electron Ions

330 formula(e) evaluated with 1 results within limits (up to 50 closest results for each mass)

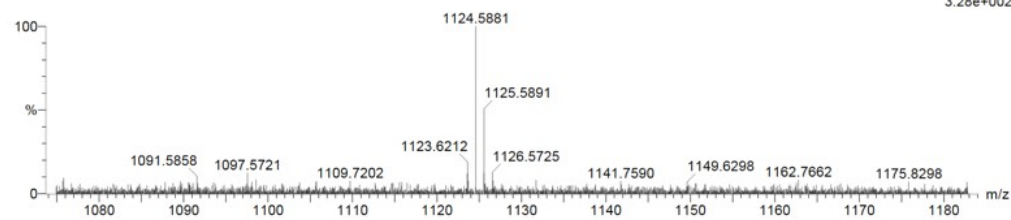
Elements Used:

C: 63-63 H: 0-99 N: 0-5 O: 0-10 F: 0-5 B: 2-2

CC-ZHAO

ZC-CN-21 31 (0.359) Cm (30:45)

1: TOF MS ES+
3.28e+002



Minimum:

Maximum:

Mass Calc. Mass mDa PPM DBE i-FIT i-FIT (Norm) Formula

1124.5881 1124.5903 -2.2 -2.0 27.5 199.4 0.0 C63 H78 N5 O10 F2 B2

Figure S21. HRMS spectrum of compound aza-BOD-B1

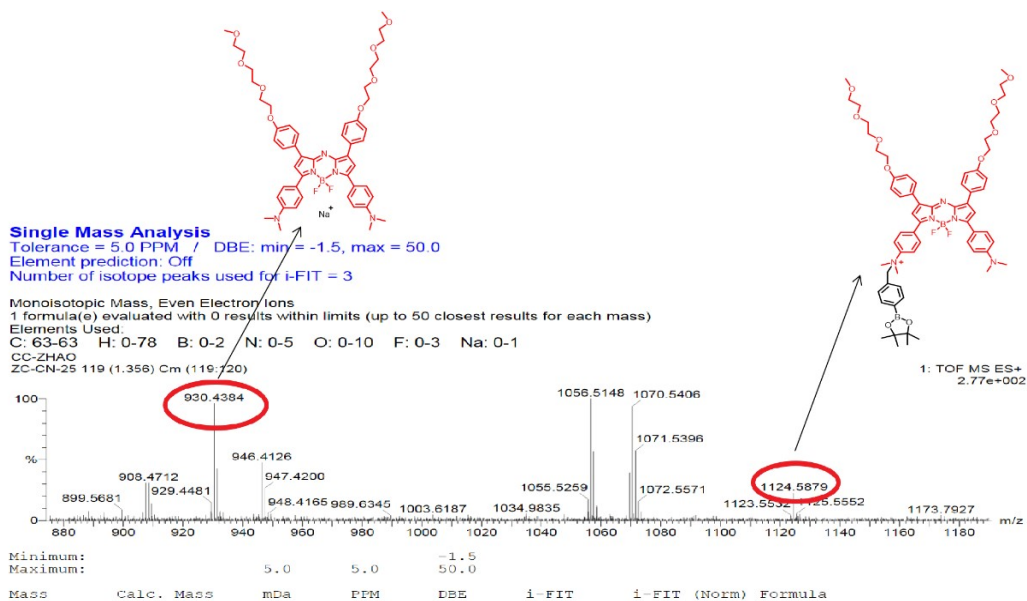


Figure S22. HRMS analysis for demonstration of the conversion of aza-BOD-B1 to aza-BODIPY-1 in the presence of H₂O₂.

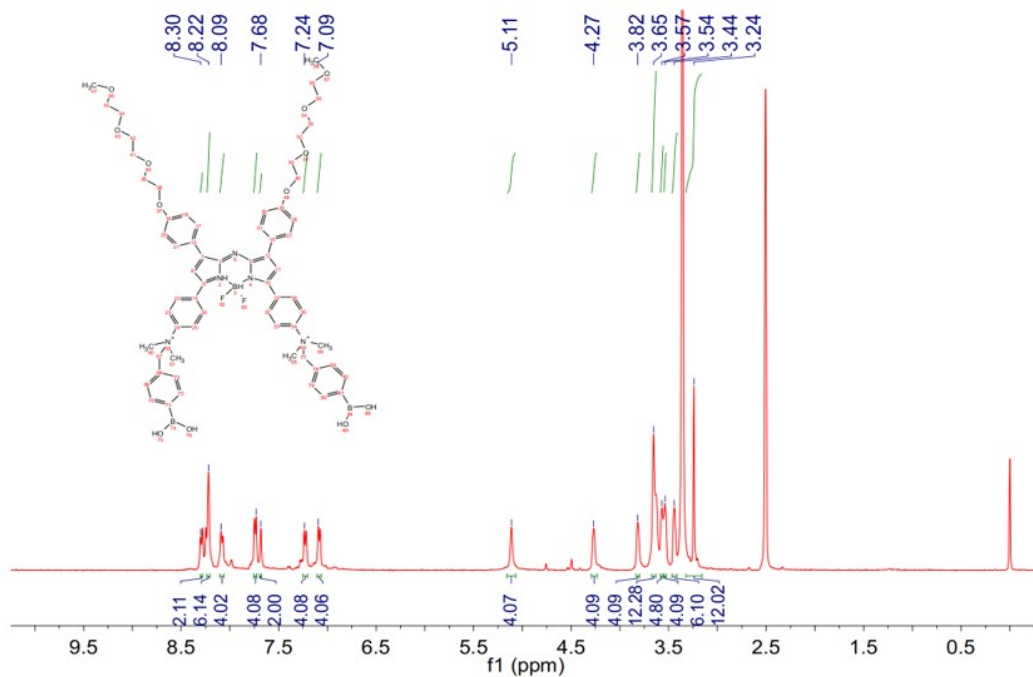


Figure S23. ¹H NMR (DMSO-*d*₆, 400 MHz) spectrum of compound aza-BOD-B2

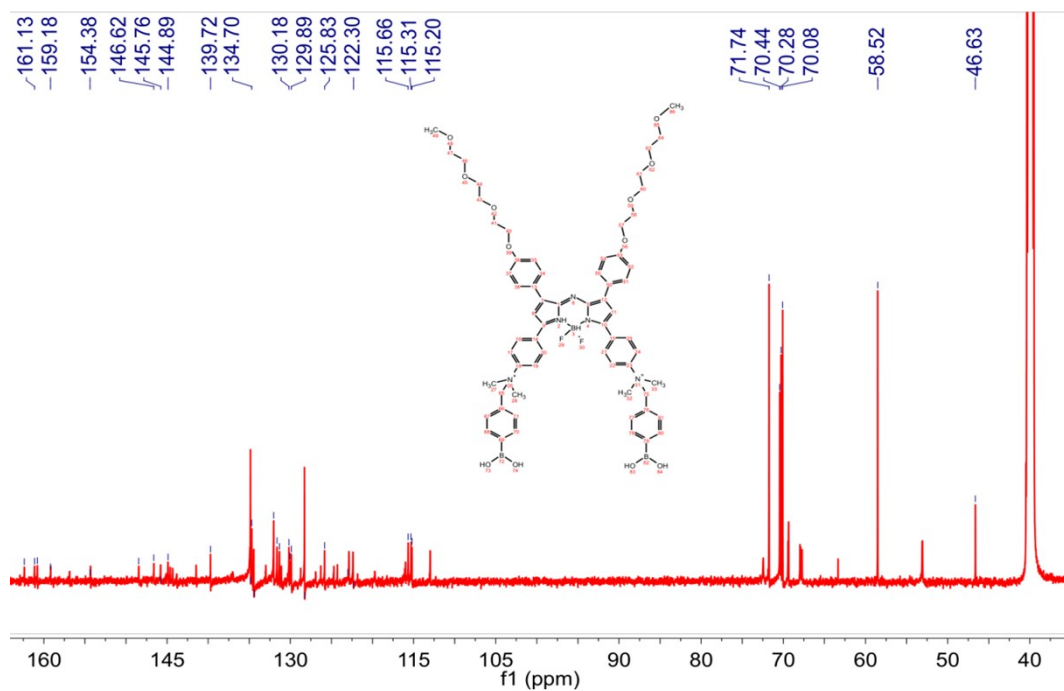


Figure S24. ^{13}C NMR ($\text{DMSO-}d_6$, 600 MHz) spectrum of compound aza-BOD-B2

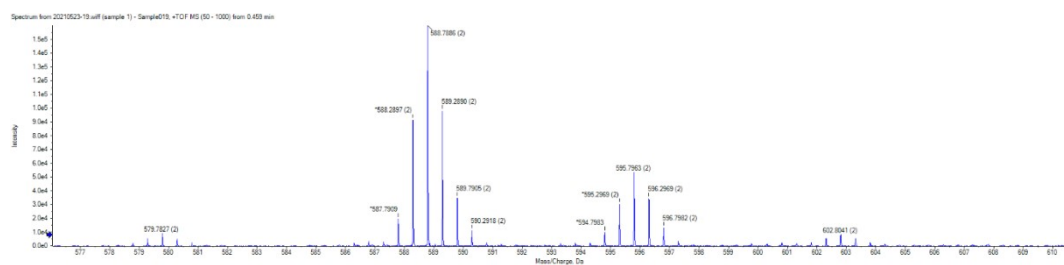


Figure S25. HRMS spectrum of compound aza-BOD-B2

References

- [1] D, Roper, W. Ahn, M. Hoepfner, *J. Phys. Chem. C*, **2007**, *111*, 3636.